

Electronic Supporting Information

Materials Used

Reagents used for synthesis were: active carbon Vulcan® XC72R GP-3921 (Cabot); palladium nitrate ($\text{Pd}(\text{NO}_3)_2$; 12-16% w/w Alfa Aesar); lithium acetate dihydrate ($\text{Li}(\text{OAc})_2 \cdot 2\text{H}_2\text{O}$ reagent grade, Sigma-Aldrich); butyllithium solution (2.5M in hexanes, Sigma-Aldrich); tetrahydrofuran (THF), anhydrous, $\geq 99.9\%$, inhibitor-free, Sigma-Aldrich); 1-butanol (anhydrous, 99.8%, Sigma-Aldrich); Ethanol (puriss. p.a., absolute $\geq 99.8\%$ (GC), Sigma-Aldrich); borane-THF complex (1M, anhydrous, Sigma-Aldrich)

Gases were supplied in cylinders by BOC: acetylene (10.29% in nitrogen), H_2 (compressed hydrogen), N_2 (oxygen free compressed nitrogen), CO (Carbon monoxide CP grade 100%).

Experimental Section

Synthesis of 5% Pd on Carbon: Vulcan® carbon (approximately 1.9 g) was placed in a round-bottom flask equipped with a stirrer bar. To the flask $\text{Pd}(\text{NO}_3)_2$ solution in nitric acid (210.25 g mL^{-1} , 0.48 mL, 2.283 mmol) were added along with but-1-ol (100 mL). The reaction was stirred at room temperature overnight. The raw product, a caked black powder, was then filtered over a Büchner funnel and washed with deionised water (400 mL), then with ethanol (400 mL).

Reduction and Calcination of 5% Pd on Carbon: 5% Pd/C was reduced in a tube furnace (Carbolite) under a flow of a 1:1 mixture of hydrogen and nitrogen gases with a total flow rate of 60 mL min^{-1} . The furnace was heated up to 550°C at a ramp rate of $10^\circ\text{C min}^{-1}$ and held at the final temperature for 3 hours, before being left to cool to room temperature. Before removing the catalyst from the furnace, it was left under only nitrogen flow for 15 minutes.

Synthesis of $\text{Pd}^{\text{int}}\text{Li/C}$: Pd/C nanoparticles (synthesised above, 100 mg) and lithium acetate dihydrate (73 mg, 0.714 mmol) were accurately weighed out and ground together using an agate pestle and mortar for 5 minutes until a homogeneous mixture of the two powders was obtained. This mixture was then transferred to a three-necked round bottom flask fitted with a stopper and a gas bubbler, which was then attached to a nitrogen gas line. Under N_2 the reaction was heated to 250°C for 2 hours. This was followed by washing with water (200 mL) and ethanol (400 mL) before being left to dry overnight.

Synthesis of $\text{Pd}^{\text{int}}\text{B/C}$: Synthesis taken from Chan *et al.*¹ Pd/C nanoparticles (synthesised above, 100 mg) were placed in a three-necked round bottom flask were suspended in tetrahydrofuran (THF) (3 mL) under N_2 prior to the addition of BH_3 -THF complex solution (2 mL). The resultant suspension was heated to 40°C to evaporate the solvent. Once evaporated the black powder is heated to 200°C for one hour. After cooling to room temperature the sample is washed with water (200 mL) and ethanol (200 mL) before leaving to dry overnight.

Thus, at present, a fixed but large excess of the dopant above to the above synthesis was used to ensure some degree of octahedral holes filling of the palladium nanoparticles in reproducible manner since other uptakes i.e. from support and particle surface as well as their slow diffusion to interstitial to the deeper part of crystals can complicate the systematic variation of loading. From lattice expansions the obtained 13.7% octahedral holes filling for Li and 15% for B seem to be the maximum loadings. Our preliminary work using lower amounts of the dopants gave some areas of unmodified Pd with no interstitial filling but other areas of heavy filling, etc (TEM). It was possible to selectively remove some dopants from external surface using acid wash. But, so far, we are not yet able to control the optimal doping to the crystals in a reproducible and meaningful manner. ICP/EDX analysis are unable to reflect the actual Li or B contents in Pd particles during handling and catalysis since there are couple of drawbacks. First, carbon support and Pd particle surface are shown to retain some Li and B from the synthesis and secondly, if the interstitial Li or B atoms left the lattice they may interact with them. Therefore, taking Li or B measurements in entirety may not reflect the truth contents as interstitial or surface B/Li species.

$\text{CO}/\text{C}_2\text{H}_2$ Chemisorption: Small samples of the catalyst (approx. 20 mg) were placed in a Quantachrome Instruments ChemBET Pulsar TPR/TPD automated chemisorption analyser. All samples were heated to 100°C for 15 minutes under hydrogen before being cooled to 30°C under an inert gas (N_2 or He) before a minimum of 7 titrations with the titrant gas.

Characterisation: Powered X-ray diffraction (XRD) patterns were obtained on a PANalytical X'Pert Pro diffractometer operating at 40 kV and 30 mA. *In-situ* XRD patterns were obtained on a Siemens D5000 X-ray diffractometer operating at 40 kV and 40 mA. Powders were slowly heated up to 500°C with XRD profiles collected at 50, 100, 150, 200, 220, 240, 260, 280, 300, 320, 340, 360, 380, 400, 450, and 500°C as well as 30°C after cooldown.

Temperature programmed reductions (TPR) were run on a CE Instruments Thermoquest TPDRO 1100 machine

Degree of Octahedral Hole Filling.

In order to estimate the degree of lithium filling in the interstitials within the palladium lattice, the I15 Beamline, Diamond Light Source was utilised. This X-rays beam has a wavelength, $\lambda = 0.16314 \text{ \AA}$ with correspondingly large energy (76.0 keV). Using Rapid Acquisition Pair Distribution Function method, it is possible to measure the distances between atoms within this sample.² The data points were thus corrected for all interferences, normalised, and converted into an integrated one-dimensional pattern from the original two-dimensional source and are shown in Fig. S1. The data was refined in PDFgui, in which scale factor, lattice parameters, dampening and broadening factors were set to be refined, with the fit range set to be from 1.5 to 10 \AA .⁴⁰ After building a model in PDFgui with lithium occupying a set percentage of the octahedral sites, the best fit was found with 13.7% of the octahedral sites filled with lithium. In a theoretical study Gelatt Jr. *et al.* had proposed that there would be a 0.1 electron transfer from Li to Pd in Pd^{-int}Li, which would equivalent to approximately 10 % of the sites filled.³ Such fitting gave a theoretical expansion of the palladium lattice, which matched well with experimental scattering values of 3.9106 to 4.0053 \AA . In control experiment, unmodified 50 % Pd/C sample gave a slightly larger lattice parameter than would be expected of bulk palladium (3.89 \AA) although it matched the lattice parameter of 3.91 \AA of the α phase of palladium with disorders.⁴ Interestingly, the unmodified Pd/C sample gave an additional tiny peak in the interstitial position, which might be due to the presence of oxygen from air, or some residual carbon.

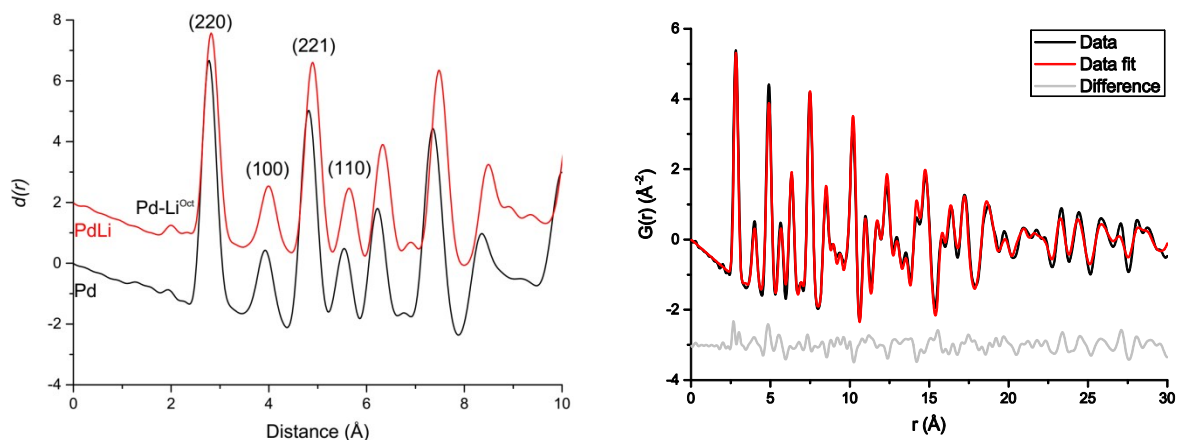


Fig. S1: (a) left-PDF patterns of 50 % Pd/C (black) and 50% Pd^{-int}Li/C (red). The positions of the (220), (100), (221) and (110) Miller indices are highlighted. (b) right- data fitting of experimental Pd^{-int}Li/C (black) to theoretical value (red). A simple crystal model is based on Li⁺ placing in octahedral sites of Pd fcc lattice. The data was collected over the range $0.5 < Q < 50 \text{ \AA}^{-1}$. This was corrected for background, Compton and multiple scattering, and beam attenuation by the sample holder interference by the GudrunX package. GudrunX also took the one-dimensional pattern, generated by the DAWN software from the two-dimensional source, and normalised it to the normalised structure factor ($S(Q)$), and hence, by using Keen's method, outputted the PDF as a $d(r)$ function.⁵⁻⁷

In-situ XRD in air.

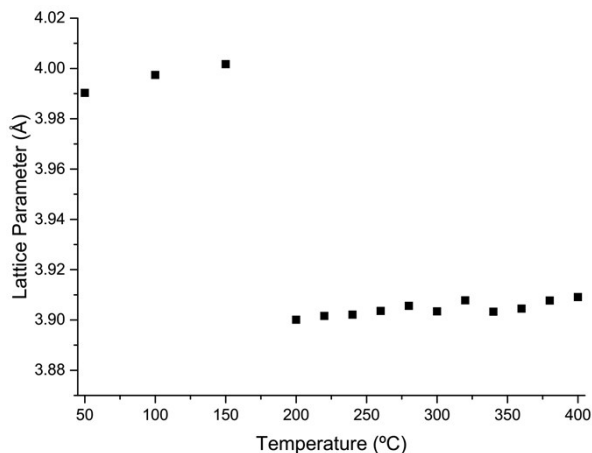


Fig S2: The variation lattice parameter a_0 with temperature for Pd^{-interstitial}Li/C.

From temperature-dependent *in-situ* powder X-ray diffraction, it is discernible that the material Pd^{int}Li/C Vulcan is stable in air flow up to and including a temperature of 150°C (Fig. S2). The lattice parameter increases from an initial 3.99 Å to 4.00 Å at 150°C before decreasing to 3.90 Å at 200°C. The latter value is very close to the observed lattice parameter of 3.89 Å for unmodified Pd/C. It can thus be concluded that the material is stable in air up to at least 150°C, before then detercalating at higher temperatures.

CO chemisorption.

All samples were titrated with the titrant gas a minimum of seven times in order to accurately determine their metal surface areas, the peaks were integrated and converted to number of metal active sites, assuming 1 atom of adsorbed gas = 1 metal active site. The gas used was 100% CO, supplied by BOC.

Table S1: Summary of the observed metal surface area's as calculated by CO chemisorption in terms of area per gram of catalyst and area per gram of palladium.

Sample	Surface Area (m ² g _{cat} ⁻¹)	Surface Area (m ² g _{Pd} ⁻¹)
5% Pd/C	1.244	24.788
5% Pd ^{int} Li/C	1.131	22.543
5% Pd ^{int} B/C	1.015	20.238

The samples are washed as part of the synthesis (ensuring no lattice re-contraction) to remove excess dopers from the Pd particle surface otherwise boron oxide, lithium oxide/carbonate and other phases can be present in XRD. We have been reluctant to wash more extensively due to the potential risk of leaching the interstitial dopant out of the lattice. As a result, some degree of their surface coverages might have given the small differences in their measured surface areas as seen in Table S1. However, the differences in surface area have been normalized and accounted for in our acetylene hydrogenation testing.

Catalytic Hydrogenation

Hydrogenation experiments were carried out in a fixed-bed continuous flow reactor fitted inside of a tubular furnace. Either 75 mg (H rich conditions) or 5 mg (incomplete conversion) of catalyst were placed between two plugs of quartz wool into a Pyrex glass tube of 4 mm internal diameter before fitting into a tubular furnace. The ends of the glass reactor tube were connected to an inlet for the reagent gases (mixed H₂, N₂ and C₂H₂ with flow rates controlled by mass-flow controllers and a total volume flow of 50 ml min⁻¹), and an outlet for the product gases attached to a Perkin Elmer AutoSystem XL Gas Chromatograph (GC). The GC was fitted with a HayeSep T column and a thermal conductivity detector. Five gas chromatograms (Fig S4) were obtained for each temperature point, after having waited for at least 30 minutes for gas flows and temperatures to reach equilibrium.

The responses from the TCD detector in the gas chromatograph were converted into percent yields from the product gas mixture, from this, the composition of the product gas mixture could be determined. Typically, the carbon balance of the reaction did not equal 1 (typically 0.90 to 0.98), the small discrepancy attributed to C fragments or C4 polymerisation products.

Testing under Industrial mixture

Under industrial acetylene hydrogenation conditions (feedstream conditions: acetylene 1%; hydrogen 1.1%; ethylene 97.9%). Both acetylene conversion and final ethane concentration are tracked. This is done because the feed is rich in ethylene and therefore it is very difficult to track precisely the amount of ethylene is being produced. The problem is not that the acetylene (and therefore the ethylene that is being produced) is very low, but it is low compared to the concentration of ethylene already in the feed. The reaction temperature parameters are varied to obtain data through the whole range of conversion for each catalyst.⁸ Plotting the results against conversion has the effect of removing variations in the testing conditions as a factor in catalyst performance. In the industrial setting it is key to maximise acetylene conversion, whilst minimising the concentration of ethane downstream. If a significant amount of acetylene remaining in the feed, downstream processes like ethylene polymerisation are adversely effects. On the other hand, should there be a larger amount of over-hydrogenation this is economically inefficient.^{9,10} The results are summarised in Fig. S3.

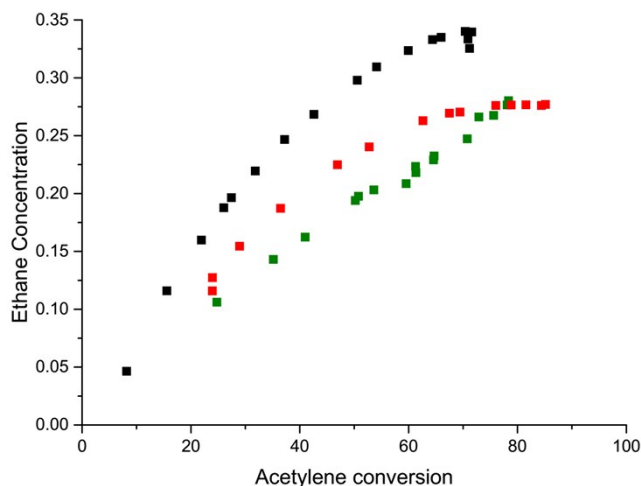


Fig. S3: The comparison between down-stream ethane concentration and acetylene conversion for the three catalysts under industrial testing conditions. The black is Pd/C, green Pd^{-int}B/C and Pd^{-int}Li/C is red.

Modelling

The bottom two layers were frozen and the top layers allowed to relax (Fig. S4). Two structural models were examined for the interstitial dopant elements (B and Li), one with the dopant placed on the metal surface, the other model with the dopant located in the subsurface.

$$E_{\text{seg}} = E_{\text{onsurf}} - E_{\text{subsurf}} \quad (1)$$

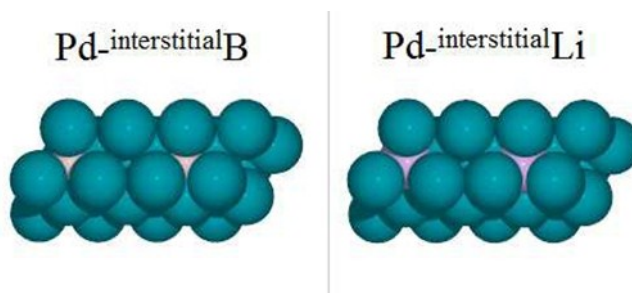


Fig. S4: Top view of the Pd(111) unit cells after relaxation. Visible within the Pd lattice are B (pink) and Li (purple).

The segregation energy (E_{seg}) (as defined in Equation 1) can be used to study the stability of the interstitial atom by comparing the relaxed energies with the dopant within the lattice (E_{subsurf}) to the dopant on the surface (E_{onsurf}). E_{seg} for the Pd^{-int}B system was positive, (+1.4 eV) suggesting that it is more stable than the Pd^{-int}Li system which was found to be metastable ($E_{\text{seg}} = -1.85$ eV). From this it would be expected that Pd^{-int}B/C would exhibit greater thermal stability than Pd^{-int}Li/C. This is what was seen experimentally through *in-situ* XRD, where Pd^{-int}Li/C is stable to 150°C whereas Pd^{-int}B/C is stable in air to 200°C.⁶

Table S2: A summary of the d band centre and Bader analyses for the positions of the d band and the charges of the individual dopant elements in the studied systems. All numbers are relative to an unmodified Pd slab and are in eV.

System	d band centre	d band width	ΔE_f	Bader Charges
Pd ^{-int} B	-0.4	+0.1	+0.03	B: +0.4
Pd ^{-int} Li	+0.2	-0.2	+0.06	Li: +0.8

Table S2 above shows the Bader and d-band analysis on the studied systems. The analyses show the net change in the d band's centre and width is more pronounced than the change in the position of the Fermi level (ΔE_f).¹¹ This is small for all systems, corroborating that this effect would be hard to detect through Pd 3d peak shifts observed in XPS. Despite the charged nature of the dopants, it is worth noting that no significant oxidation or reduction of palladium occurred. Bader analysis of the host metal showed a net change of ± 0.03 electrons, within error of no net change. As expected, we can qualitatively see that lithium modification behaves markedly differently to the boron system. Bader analysis shows that the interstitial lithium has a significantly larger charge, suggesting that it is present as an ion. However, it is notable that the compensating negative charge does not result in a localised charge on a neighbouring Pd atom, the compensating negative charge is instead delocalised across all of the Pd in the system, such that each Pd is effectively charge neutral.

In general, when a light atom is inserted interstitially into a metal lattice, it is expected that the d-band centre will narrow and increase in energy, due to the increased lattice parameter reducing the effective overlap of Pd d orbitals. The fact that lithium has no p-orbitals to interact and stabilise the transition metal d-orbitals causes a narrowing (d-band width -0.2 eV) and raising of the d-band (d-band centre $+0.2$ eV) (Table S2). Fig. S5 depicts the density of states of the d band for: unmodified palladium, the Pd-^{int}Li system, and an expanded palladium lattice (the density of states of Pd with the Li atom removed, but the geometry fixed to 3.99 Å). This allows us to separate out the influence of lattice expansion and electronic transfer due to the presence of Li. It can clearly be seen that the majority of the narrowing and broadening of the Pd d-band is a result of the increasing outermost Pd-Pd bond distances. This is caused by the interstitial location of Li; despite this the overall contribution of lithium's orbitals is relatively minor. Indeed, it is possible to view the Pd-^{int}Li system as having 'undercoordinated' lithium within the metal lattice. The stabilisation of the lithium within the lattice is not coming from an orbital overlap, but rather a charge-transfer from lithium to the palladium host. Gelatt Jr. and co-workers calculated in 1983 that there would be very little orbital overlap between Li and Pd, but that the system would still be theoretically stable.³

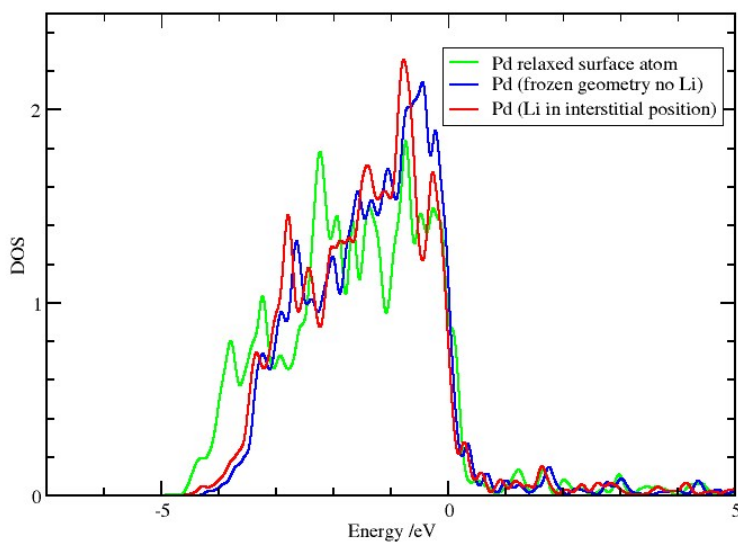


Fig. S5: Density of states for the Pd surface during Li absorption, green: fully relaxed system with no Li absorbed, red: Li interstitially located, blue the frozen geometry of the Pd-^{int}Li system with the Li removed (as an indicator of the influence of lattice distortion due to Li).

References

- 1 C. W. A. Chan, A. H. Mahadi, M. M.-J. Li, E. C. Corbos, C. Tang, G. Jones, W. C. H. Kuo, J. Cookson, C. M. Brown, P. T. Bishop and S. C. E. Tsang, *Nat. Commun.*, 2014, **5**, 5787.
- 2 P. J. Chupas, X. Qiu, J. C. Hanson, P. L. Lee, C. P. Grey and S. J. L. Billinge, *J. Appl. Crystallogr.*, 2003, **36**, 1342–1347.
- 3 C. D. Gelatt, Jr., A. R. Williams and V. L. Moruzzi, *Phys. Rev. B*, 1983, **27**, 2005–2013.
- 4 A. Rose, S. Maniguet, R. J. Mathew, C. Slater, J. Yao and A. E. Russell, *Phys. Chem. Chem. Phys.*, 2003, **5**, 3220–3225.
- 5 A. K. Soper and E. R. Barney, *J. Appl. Crystallogr.*, 2011, **44**, 714–726.
- 6 D. A. Keen, *J. Appl. Crystallogr.*, 2001, **34**, 172–177.
- 7 M. Basham, J. Filik, M. T. Wharmby, P. C. Y. Chang, B. El Kassaby, M. Gerring, J. Aishima, K. Levik, B. C. A. Pulford, I. Sikharulidze, D. Sneddon, M. Webber, S. S. Dhesi, F. Maccherozzi, O. Svensson, S. Brockhauser, G. N ray and A. W. Ashton, *J. Synchrotron Radiat.*, 2015, **22**, 853–858.
- 8 F. Studt, F. Abild-Pedersen, T. Bligaard, R. Z. S rensen, C. H. Christensen and J. K. N rskov, *Science*, 2008, **320**, 1320.
- 9 J. Osswald, K. Kovnir, M. Armbruster, R. Giedigkeit, R. Jentoft, U. Wild, Y. Grin and R. Sch gl, *J. Catal.*, 2008, **258**, 219–227.
- 10 J. Osswald, R. Giedigkeit, R. Jentoft, M. Armbruster, F. Girgsdies, K. Kovnir, T. Ressler, Y. Grin and R. Sch gl, *J. Catal.*, 2008, **258**, 210–218.
- 11 G. Henkelman, A. Arnaldsson and H. J nsson, *Comput. Mater. Sci.*, 2006, **36**, 354–360.